MONK10: A Monte Carlo Code for Criticality Analysis

**David Long, Simon Richards, Paul N Smith, Christopher Baker, Adam Bird, Nigel Davies,
Geoff Dobson, Tim Fry, David Hanlon, Ray Perry and Max Shepherd**
Amec Foster Wheeler, Clean Energy, NE & CIS
Kings Point House, Queen Mother Square, Poundbury, Dorchester DT1 3BW, United Kingdom
david.long@amecfw.com; paul.smith3@amecfw.com; simon.richards@amecfw.com

ABSTRACT

The MONK® code, if we include its predecessor GEM, has now been in use for 50 years. It is a Monte Carlo code for nuclear criticality and reactor physics analyses which is used extensively in the UK nuclear industry and worldwide. In 2014 a major new version of the code, MONK10A, was released introducing many new features; these are described with example applications presented where appropriate. Experience with MONK9A models indicates that MONK10A has increased run-time performance for all cases and on average runs 2.4 times faster.

New geometry options include the direct import of CAD generated models using the new IGES body, POLY body, TETMESH Hole and TETMESH Zone features. Example calculations for a selection of CAD import options are presented and compared with the intrinsic MONK geometry representation, with relative merits discussed.

New Features are included to assist with the modeling of distributed parameters; such features include Unified Tally (UT), Action Tallies (AT) in UT and Shannon entropy. The latter is useful in assessing the convergence of distributed parameters, such as scalar neutron flux. As such it is an important tool in determining the appropriate point to stop settling and begin scoring stages in a Monte Carlo simulation. The utility of UT, AT-in-UT and Shannon entropy is demonstrated using calculations employing the new CAD import geometry options. Runtime Doppler broadening is included to allow accurate representation of temperature distributions within models. Example calculations which further demonstrate UT and AT-in-UT are presented for different bodies at different temperatures to evaluate the effects of temperature differences on k-effective and reaction rates.

The MONK10A code was issued with a new set of continuous energy and group nuclear data libraries. These include JEFF3.1, JEFF3.1.1, JEFF 3.1.2, ENDF/B-VII.0 and CENDL 3.1 libraries. The inclusion of a range of libraries allows the user to evaluate the impact of different international nuclear data evaluations on their results and an example is provided to illustrate the differences that can arise from the use of different nuclear data evaluations. The code was also issued with a new version of the VisualWorkshop IDE to allow easy construction and editing of input decks, running of calculations and display of geometry and results. Examples are provided of the geometry and results display and showing how results can be superimposed upon the geometry.

1. INTRODUCTION

MONK10A was released in 2014 as a major update to the UK nuclear industry standard Monte Carlo nuclear criticality safety analysis code.

The new features in MONK10A [1] include:
- additional input, control, parameter and looping features;
- new Fractal Geometry (FG) options;
- new Hole geometries (employing Woodcock tracking);
- CAD import;
- new action tallies; Unified Tally (UT) scoring; action tallies in UT meshes;
- new sensitivity options; data assimilation (ADJUST option);
- Shannon entropy;
- a fixed source option for modelling sub-critical systems with external sources;
- run-time Doppler broadening;
- new energy group schemes;
- material and energy dependent fission spectrum (WIMS);
- new nuclear data evaluations in continuous energy and broad group formats;
- mesh-based burn-up option; and
- parallel processing.

In this paper we present examples demonstrating the use of the new tally capabilities for scoring distributed quantities such as reaction rates, and the use of Shannon entropy as a metric for assessing source convergence. Also demonstrated is the import of CAD models in a range of different formats, and comparison of the results of those models with the equivalent geometry modeled in the native MONK FG format.

It should be noted that MONK10A run-times have been compared with those from MONK9A using the MONK validation database, consisting of 820 models. In all cases MONK10A ran significantly quicker than MONK9A, with run-times ranging between 1.6 to 3.7 times faster. On average MONK10A was 2.4 times faster than MONK9A. Additional large increases in the performance of MONK10A calculations can also be achieved using the new parallel processing capability.

2. Unified Tally and Action Tallies Modules

The new Unified Tally (UT) module in MONK10A allows the user to score the scalar neutron flux in a gridded mesh independent of the geometry model. Each UT mesh has a shape defined by some of the simple bodies available in the existing FG package, and can take any position or orientation within the model geometry. The size of each scoring region within the UT mesh is defined through subdividing the containing body shape according to its defining parameters. Any number of UT meshes can be defined and may overlap freely. The scalar neutron flux is scored within a UT body using either track length or collision density estimation and can be obtained across user defined energy groups. Optionally the scored fluxes may be decomposed by material.

In addition to scoring the neutron scalar flux the new AT-in-UT (action tally in unified tally) module allows the user to score action tallies within a defined UT mesh for the following reactions:
- capture
- fission and number of fission children
- elastic scatter

- inelastic scatter
- (*n,2n*) and (*n,3n*)

The scoring of each AT-in-UT reaction and their standard deviations can be requested for the total or each subdivision of the specified UT body and across user defined energy groups. Scoring can also be restricted to selected materials or nuclides within the UT body. The scoring results for AT-in-UT can be requested to be the absolute tallies of each reaction or normalized to 10,000 samples.

3. Shannon Entropy Module

When scoring distributed parameters in 3-Dimensional spatial meshes, such as the scalar neutron flux or reaction rate tallies, it is essential that such quantities have converged (from the initial fission source estimate) before scoring commences [2]. Estimates of distributed parameters typically require a greater number of samples than those needed to estimate *k*-effective [3]. Therefore the convergence and stochastic uncertainty of *k*-effective alone are not sufficient criteria for determining the source convergence of distributed parameters, which must be determined independently to the convergence of *k*-effective.

A useful diagnostic for determining the source convergence of distributed parameters is the Shannon Entropy [4]. The Shannon entropy is a well-known concept from information theory which characterizes (in terms of uniformity) the distribution of a parameter field to a single scalar value, which can then be readily compared through successive stages to assess convergence. Within MONK10A it is possible for the user to determine the Shannon Entropy (H_ϕ) of the scalar neutron flux within a defined UT mesh given by [5],

$$H_\phi = -\sum_{j=1}^{N} p_j \log_2(p_j) \qquad (1)$$

Here p_j is the fraction of the total flux (or probability) appearing in cell *j* of the defined UT mesh and *N* is the total number of UT mesh cells. The magnitude of the Shannon entropy will therefore converge to a single steady-state value as the neutron flux convergences to a stationary value. A potential undesirable property of the Shannon entropy based on the above equation is that its absolute value is dependent on the total number of grid cells *N* defined in the superimposed UT mesh. To overcome this dependence the MONK10A user can request a modified value of Shannon Entropy given by,

$$H'_\phi = H_\phi - \log_2 N \qquad (2)$$

As for both UT and AT-in-UT scoring, the Shannon Entropy of neutron flux over a UT mesh can be obtained across user defined energy groups.

4. CAD Import Options

Historically, models of the critical systems are generated within MONK using the intrinsic geometry package, which consists of two complementary components: Fractal Geometry (FG) and Hole Geometry. The FG component uses text-based Constructive Solid Geometry (CSG) for defining the union, difference and intersection of simple mathematical bodies, including the sphere, box, rod, prism, cone and torus to assemble structured parts of a model independently to the entire system. Structured model parts can then be combined, in the same manner, to form more complex parts until the entire model geometry is assembled. The Hole Geometry package is used in conjunction with FG to facilitate the specification of more complicated objects with complex geometrical detail, which are impossible to model in FG using simple bodies, and to expedite the definition of commonly replicated shapes.

It has become common place for criticality assessors to create geometrical models within MONK through interpreting engineering drawings generated by a Computer Aided Design (CAD) package, converting such drawings to text-based FG and/or Hole Geometry input. The conversion process can be tedious, time consuming and requires detailed verification since it is prone to human error. This approach to critical system design can therefore result in long iteration times (increasing cost) between the initial generation, assessment and revisions of geometries when developing a model. The direct use of CAD files within MONK10A negates the need to interpret and convert CAD geometries to text-based input and therefore has the potential to optimize the design process, reducing user effort (decreasing cost) and improving quality assurance. In addition to these benefits, the direct use of CAD files also extends the range of geometrical objects available to the MONK10A user since CAD packages can generally represent any arbitrary shape, while the FG and Hole Geometry packages, powerful as they are, cannot.

In MONK10A it is now possible to define model geometries through the direct import of CAD files. CAD models can be imported within the existing FG package using the new IGES body, POLY body and TETMESH zone features [6,7,8]. CAD models can also be imported within the Hole Geometry package using the new TETMESH hole. A brief discussion on the details and relative merits of each method are presented below.

4.1. IGES Body

The Initial Graphics Exchange Specification (IGES) is an engineering industry standard file format for transferring 3-Dimensional models between different CAD packages. CAD models exported in the IGES file format can be directly imported into certain structured FG parts of MONK10A using the new IGES body feature. The IGES body option is provided in MONK10A as an evaluation feature. It is recommended that IGES files imported into MONK10A are generated using the Solidworks or Autodesk Inventor CAD software packages, other CAD packages maybe used but have not been tested. The IGES import option provides full and accurate support for the range of geometry capabilities offered by CAD packages with no geometrical approximation or void spacing. Compared to models represented by solid or surface meshing techniques, such as the POLY body and TETMESH features, the IGES import option avoids problems such as large memory costs and the need to perform mesh generation which can be time consuming and complex.

4.2. POLY Body

CAD models exported in triangular polygon surface format can be directly imported into MONK10 using the POLY body feature, where model geometries are represented by a mesh of triangular facets formed from a set of numbered triplet nodes defined by their coordinates. The POLY body currently supports triangular polygon surface representations from models exported in STL format and OBJ format via a translator provided in VisualWorkshop (additionally, tetrahedral mesh files in the format for the TETMESH features can be translated to the polygon surface representation of the POLY body using a translator provided in VisualWorkshop). The POLY body import option is also provided in MONK10 as an evaluation feature. The POLY body is a fully integrated FG body in MONK10A and as such is supported by the wireframe and ray-trace views in VisualWorkshop (the IGES import option is only supported by the ray-trace view). Since the POLY body mesh only represents geometrical surfaces the memory cost is lower when compared to the solid mesh of the TETMESH feature and models are efficient to load. Particle tracking through the POLY body is very efficient and unaffected by the number of polygons defined in the mesh. The only disadvantage of the POLY body option is that when using a faceted polygon representation, in common with any discretised representation, there are inevitable geometric approximations to curved surfaces.

4.3. TETMESH Hole and TETMESH Zone

A CAD model represented by a solid tetrahedral mesh file can be directly imported into MONK10A using the new TETMESH Hole or TETMESH Zone features. Both features require the CAD model to be generated as an ASCII file in the format produced by ANSYS ICEM CFD. While both options read the same file format the TETMESH Hole and TETMESH Zone options import CAD models into the Hole Geometry and FG packages respectively. The TETMESH Hole is a fully quality assured feature of MONK10A. The runtime performance of the TETMESH Hole and TETMESH Zone options can be optimized at the expense of increased memory. If enough memory is available then the TETMESH import options can have comparable or better run-time performance than the POLY body option. The TETMESH Zone is useful for options which do not support Hole Geometries and is an evaluation feature within MONK10A. For the results presented in this paper only the TETMESH Hole is considered. As for the POLY body a disadvantage of the TETMESH option is the inevitable geometrical approximations made to curved surfaces when using a tetrahedral mesh representation.

5. Transport Flask Example

To demonstrate the new CAD geometry import options, the utility of the new Shannon Entropy module and the application of the new UT and AT-in-UT modules available in MONK10A we consider the example test case of a fuel transport flask. The geometry of the transport flask is shown in Fig 1. The model contains 12 cylindrical fuel rods positioned concentrically in a chamber (void) at the centre of the flask. Each fuel rod is composed of pure ^{235}U and has a hollow (void) central region. The supporting structure of the flask is composed of stainless steel with a large tank of ordinary water surrounding the fuel rod chamber.

5.1. Comparison of Geometry Options

To facilitate a comparison between the CAD import options and the text-based geometry approach the transport flask was run in MONK10A using 2000 superhistories[1] per stage with a total of 150 stages (50 settling stages to achieve source convergence and 100 scoring stages to calculate results to within). The text-based geometry of the model was constructed using the existing FG package (using the Nest and General Part structures) and required approximately 300 lines of input code within the material geometry specification unit of MONK10A, compared to approximately 5 lines for each of the CAD import options.

From Fig. 1 it is clear that the IGES import option is able to exactly replicate the model geometry of the FG case, while both the POLY body and TETMESH zone options contain a certain degree of geometrical approximation when representing the curved surfaces of the cylindrical fuel rods and containing steel structure. All four of the geometry options produced values of *k*-effective which are within three standard deviations of each other, as shown in Table I.

It is apparent that the geometrical approximations present in both the POLY body and TETMESH Hole import options do not produce statistically different *k*-effective values to the exact model representations of the FG and IGES body options. For the results presented above the POLY body mesh contained approximately 375,000 polygon surfaces and the TETMESH Hole mesh approximately 900,000 tetrahedrons. If the resolution of the meshes used in these approaches was coarsened (using lower number of polygon surfaces or tetrahedrons) then the geometrical approximations to the model geometry could be significantly large enough to impact the accuracy of the calculation.

---

[1] A superhistory comprises the histories of a source neutron and all of its fission progeny up to and including the Lth generation, where L=10 by default.
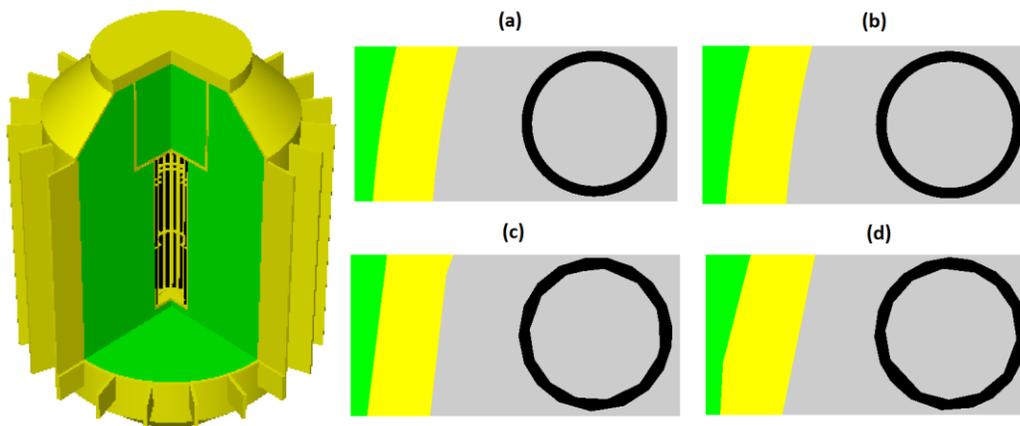
Figure 1: Transport flask model: (far left) Cut away 3D ray-trace image of entire geometry with fuel rods, stainless steel structure and water tank shown in black, yellow and green respectively. Detail 2D ray-trace images in the axial plane: (a) FG, (b) IGES body, (c) POLY body and (d) TETMESH Hole.

Table I. Calculation results for the Transport Flask model using FG and CAD import options.

Geometry Option	k-effective (-3σ)	k-effective	k-effective (+3σ)	Average Samples/Sec	Performance (FG/CAD)
FG	0.3260	0.3275	0.3290	117	-
IGES Body	0.3247	0.3262	0.3277	3	39.0
POLY Body	0.3269	0.3284	0.3299	61	1.91
TETMESH Hole	0.3270	0.3285	0.3300	38	3.08

As a metric of run-time performance Table 1 shows the average number of calculated samples per second for the transport flask model when using the FG and CAD import geometry options. A comparison of the performance between each CAD import option and the text-based FG approach is given in the final column of Table 1. Here we find that the performance of the POLY body and TETMESH Hole options are comparable to FG, with run-time performance being approximately 2 and 3 times slower respectively. The run-time performance of the IGES import option is 39 times slower than the text-based FG geometry. Improvements to the run-time performance of the IGES import option will be included in the next release update of MONK10A, with current development work showing an increased performance by two to five times.

5.2. Convergence of Neutron Flux Using Shannon Entropy

It is well known that when solving k-eigenvalue problems for critical systems using the power iteration procedure, as is performed in MONK, the convergence rate from the initial fission source estimate for the neutron flux (eigenfunction) is slower than for k-effective (eigenvalue). Before the scoring of desired quantities can proceed without bias from the initial source estimate both k-effective and the neutron flux distribution must have converged, i.e. a sufficient number of settling stages to achieve source convergence must be run within a MONK calculation. Values of k-effective determined from a neutron flux distribution which have not fully converged from the initial source estimate will therefore be inaccurate and unreliable.

To demonstrate the utility of the new Shannon Entropy module we consider the convergence of the neutron flux distribution within the transport flask model. For this example a UT mesh over the entire model geometry was defined using a box grid with five evenly spaced subdivisions along each Cartesian dimension, resulting in a total of 125 individual scoring cells within the UT mesh. The Shannon entropy values versus stage number over both the total energy range (0.0 – 15.0 MeV) and the thermal energy range (0.0 – 4.0E-07 MeV) are shown in Fig. 2 for the FG and CAD import geometry cases.
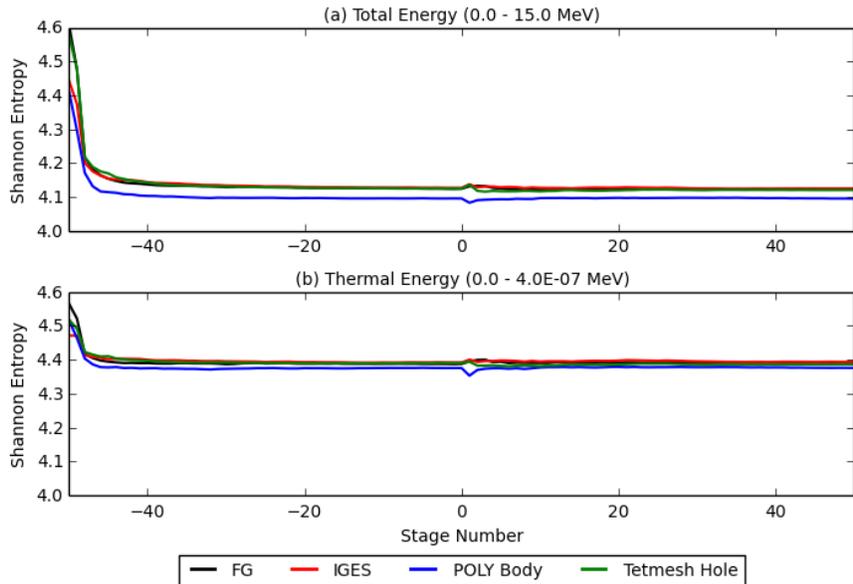
Figure 2: Shannon entropy of scalar neutron flux for transport flask model using FG and CAD imported geometries for: (a) total energy range and (b) thermal energy range.

Visual inspection of Fig.2 shows that over the total energy range the values of Shannon entropy for neutron flux have converged to a steady-state value after approximately thirty settling stages, for all geometry options considered. Employing fifty settling stages for the transport flask calculations is therefore more than sufficient to produce reliable estimates of *k*-effective, as any bias in the neutron flux distribution from the initial source estimate has been removed before scoring commences. Values of Shannon entropy over the thermal energy range also show converged behavior after approximately thirty settling stages, giving the MONK10A user additional confidence in any scored tally results within this energy range.

5.3. Thermal Elastic Scatter Using AT-in-UT

To illustrate the modeling of distributed parameters we consider the reaction counts of thermal elastic scattering within the transport flask model using the new AT-in-UT module. Here we refine the UT mesh used for calculating the Shannon entropy of the neutron flux, as described above, to allow for one hundred equally spaced subdivisions in the X and Y co-ordinate directions of our containing box. The reduced volume scoring regions of this grid provide greater resolution for results when superimposed upon the model geometry. The AT-in-UT reaction rates were requested in a user defined thermal energy group between 0.0 and 0.4 eV. The scored tallies of thermal elastic scattering events, averaged axially over the entire model, are shown in Fig. 3 as a 2-Dimensional contour plot superimposed onto the VisualWorkshop wireframe view of the geometry.

From Fig. 3 we find that the contour plots of thermal elastic scattering events are qualitatively identical for each of the geometry options considered, and show peak reaction rates in the annular region outside of the fuel chamber within the water tank as expected for this energy range. Additional confidence in the reliability of these results can be taken from the fact they are determined from a neutron flux distribution which has been shown to have converged in the thermal energy range before scoring commences, as shown by the Shannon entropy detailed in Fig. 2.
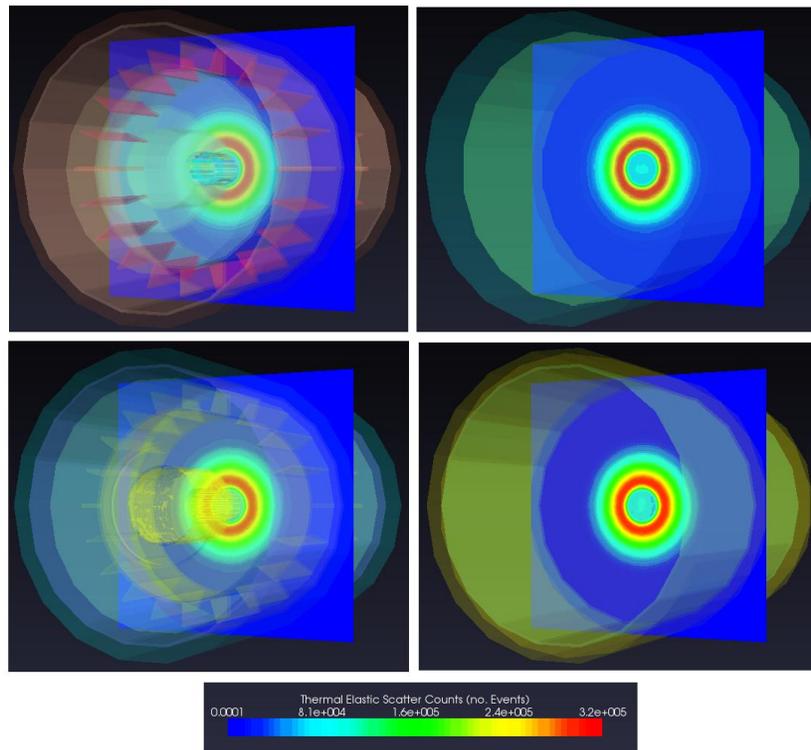
Figure 3: Thermal elastic scatter events for the transport flask model using geometries; (top-left) FG, (top-right) IGES body, (bottom-left) POLY body and (bottom-right) TETMESH Hole.

Since the POLY body option is fully integrated into the FG module it is possible to display the structure of the model in the wireframe view of VisualWorkshop, as for the FG geometry shown in Fig. 3, facilitating the analysis of the distributed tally results. This feature is unavailable for both the IGES body and TETMESH Hole options.

6. Nuclear Data Libraries

There are a variety of nuclear data libraries which are new to MONK10A; CENDL-3.1, ENDF-B/VII.0, JEF2.2, JEFF3.1, JEFF3.1.1 and JEFF3.1.2. The ANSWERS Monte Carlo packages use the BINGO file format and collision processor for these nuclear data evaluations. It should be noted that the BINGO collision processor in MONK10A has been developed to improve run-time performance when compared to the previous version in MONK9A.

It is good practice to look at a variety of nuclear data libraries to increase confidence in reported results, even if a library is not validated for a particular safety case. To demonstrate this we will show the results from calculations performed with a range of data libraries using a MONK model composed of two nested spheres, one a fissile material and the other a reflector. The fissile materials are ^{235}U, ^{239}Pu, and ^{241}Pu. The

reflector materials are ^{238}U, water and steel. The metric of comparison between results from different libraries is the number of standard deviations k-effective values are apart, defined as,

$$\frac{|k_{\text{ref}} - k_{\text{test}}|}{\sqrt{\sigma_{\text{ref}}^2 + \sigma_{\text{test}}^2}} \tag{3}$$

Here k_{ref} and k_{test} are the k-effective values from the calculations using the reference and test libraries (those being compared), which have standard deviations σ_{ref} and σ_{test} respectively. The results when comparing a variety of data libraries for different combinations of fissile and reflector material are shown in Fig. 4. Note, comparison results for the JEFF data libraries are only shown for the latest release version JEFF3.1.2.

As can be seen in Fig. 4, the cases which use ^{241}Pu provide greater differences compared to those cases which use either ^{239}Pu or ^{235}U. Differences and similarities can arise for a variety reasons. For example, some nuclear data libraries may produce similar results because they are based on the same fundamental data evaluations. The differences tend to be greater in the transuranic elements, with the exception of ^{239}Pu due to its importance in criticality safety.

One of the new features of MONK10A is the ability to adjust individual nuclear cross-sections within a particular BINGO data library using the ADJUST option. This option defines a factor by which to increase or decrease a specified reaction cross-section, or $\bar{\nu}$ (average number of neutrons produced per fission event), over a specified energy range. Here we concentrate on the adjustment of $\bar{\nu}$ and the fission cross-section which both affect the eigenvalue estimators (k-effective) of the calculation.

The ADJUST option can be used to gauge which factors within a particular library are affecting the criticality of the system, and has been used to perform data assimilation within MONK [9]. To demonstrate the new ADJUST feature we consider the results presented above when comparing the CENDL-3.1 and ENDF-B/VII.0 libraries using a ^{241}Pu fissile sphere reflected by ^{238}U. Here, the original k-effective values using ENDF-B/VII.0 and CENDL-3.1were 1.0293 and 1.0569 respectively, with the results being 13.01standard deviations apart. Using the ADJUST option the values for $\bar{\nu}$ and the fission cross section of ^{241}Pu within the CENDL-3.1 library were reduced by factors of 0.9738 and 0.960 respectively for all incident neutron energies. The adjusted calculation results for the CENDL-3.1 library, with a new comparison against the original ENDF-B/VII.0 library are shown in Table II.

Table II. Calculation results using CENDL-3.1 library with adjusted ^{241}Pu. Final column shows the comparison of adjusted results with ENDF-B/VII.0 library.

Adjustment	Factor	Adjusted CENDL-3.1 k-effective	Adjusted CENDL-3.1 – ENDF-B/VII.0 No. Standard Deviations
$\bar{\nu}$	0.9738	1.0224	3.476
Fission	0.9600	1.0279	0.660

From Table II we find that the adjustment (reduction) of both $\bar{\nu}$ and the fission cross section for ^{241}Pu within CENDL-3.1 produces smaller k-effective values, creating a closer agreement for each case between the adjusted CENDL-3.1 and ENDF-B/VII.0 libraries.

The sensitivity of k-estimators to specific material reaction cross sections within the new BINGO data libraries can be determined using the existing sensitivity data module within MONK. New to MONK10 is the ability for users to also determine the sensitivity of k-estimators to $\bar{\nu}$ for a specific fissile material. The

sensitivities of *k*-effective to $\bar{\nu}$ and fission cross-section for ^{241}Pu within the CENDL-3.1 and ENDF-B/VII.0 libraries are shown in Table III.
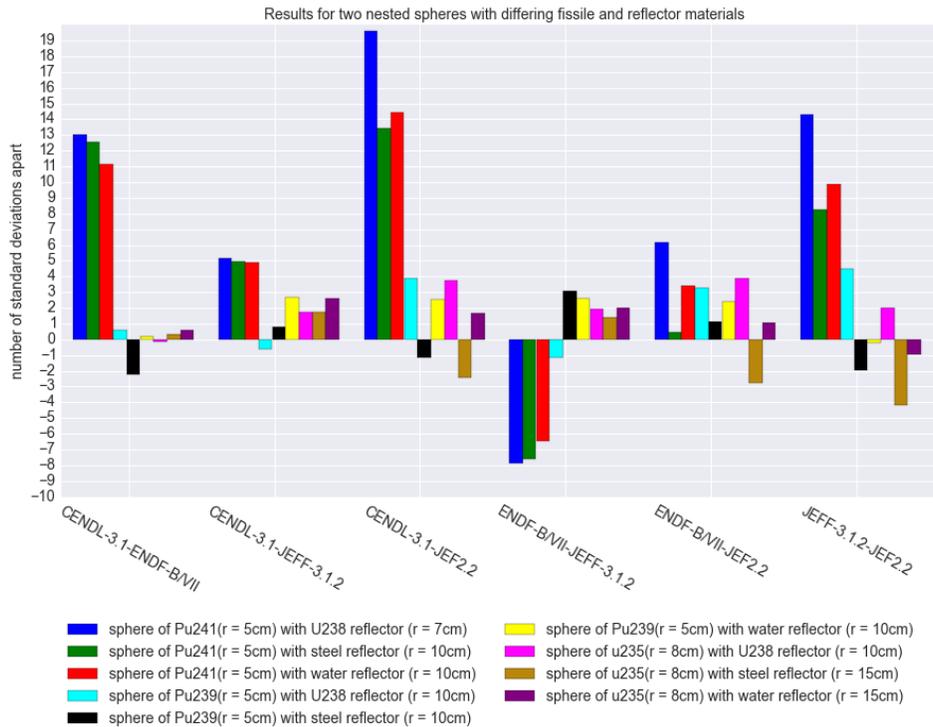
Figure 4: Nuclear data library comparison using nested spheres model with varying combinations of ^{239}Pu, ^{241}Pu and ^{235}U fissile material with ^{238}U, water and steel reflectors.

Table III. *K*-effective sensitivity results of the CENDL-3.1 and ENDF-B/VII-0 libraries to $\bar{\nu}$ and fission cross section for ^{241}Pu.

Library (Adjustment)	Sensitivity	Standard Deviation of Sensitivity
CENDL-3.1 ($\bar{\nu}$)	1.2021	0.5036
ENDF-B/VII-0 ($\bar{\nu}$)	1.1895	0.6497
CENDL-3.1 (fission)	0.6889	0.01996
ENDF-B/VII-0 (fission)	0.6917	0.01979

The results presented in Table III indicate that for both the CENDL-3.1 and ENDF-B/VII.0 libraries *k*-effective is more sensitive to $\bar{\nu}$ than fission cross section for ^{241}Pu. This result is in agreement with those presented for the ADJUST option in Table II, which show that a smaller reduction in $\bar{\nu}$ compared to the fission cross section for ^{241}Pu produces larger changes in *k*-effective when using the CENDL-3.1 data library.

7. Run Time Doppler Broadening

The BINGO nuclear libraries contain data tabulated at temperatures ranging from 293.6 to 80,000 K. In previous releases of MONK the BINGO collision processor was unable to generate data for any arbitrary temperature within this range. Instead data for the tabulated library temperature closest to the temperature requested by the user was used. Within MONK10A the BINGO collision processor has been developed to

allow Doppler broadening [10] of nuclear data cross sections to be performed at run-time during a MONK calculation, known as on-the-fly Doppler Broadening. This allows materials to be modeled at any temperature between 293.6 and 80,000 K, i.e. not restricted to the tabulated library data at specific temperatures.

Run-time Doppler broadening is available for the new CENDL-3.1, ENDF-B/VII.0, JEFF3.1, JEFF3.1.1 and JEFF3.1.2 data libraries, however it is unavailable for JEFF2.2 which uses the previous fixed temperature method (with finer, nuclide-specific, temperature tabulations). The Doppler broadening method is applied in the resolved resonance range for all nuclides present in each data library.

The impact of on-the-fly Doppler broadening is demonstrated using a PWR model based on the Hoogenboom and Martin benchmark [11], consisting of a homogeneous core with all fuel assemblies having identical construction. Since the model has 8-fold rotational symmetry a 1/8th core model was used. Two calculations were performed, the first assumed average fixed temperatures across the fuel and cladding within the assemblies of 950 K and 655K respectively, the second used an estimated temperature profile across the reactor core based on the assumption that the power profile will be qualitatively similar to that of a homogeneous cylindrical reactor (where the energy contained within the reactor for the two case was assumed to be the same). The estimated temperature profile within the reactor, shown in Fig. 5, contains peak values approaching 1010 K at the center of the core (greater than the averaged fixed values) which decrease in magnitude when moving outwards in both the axial and radial directions.
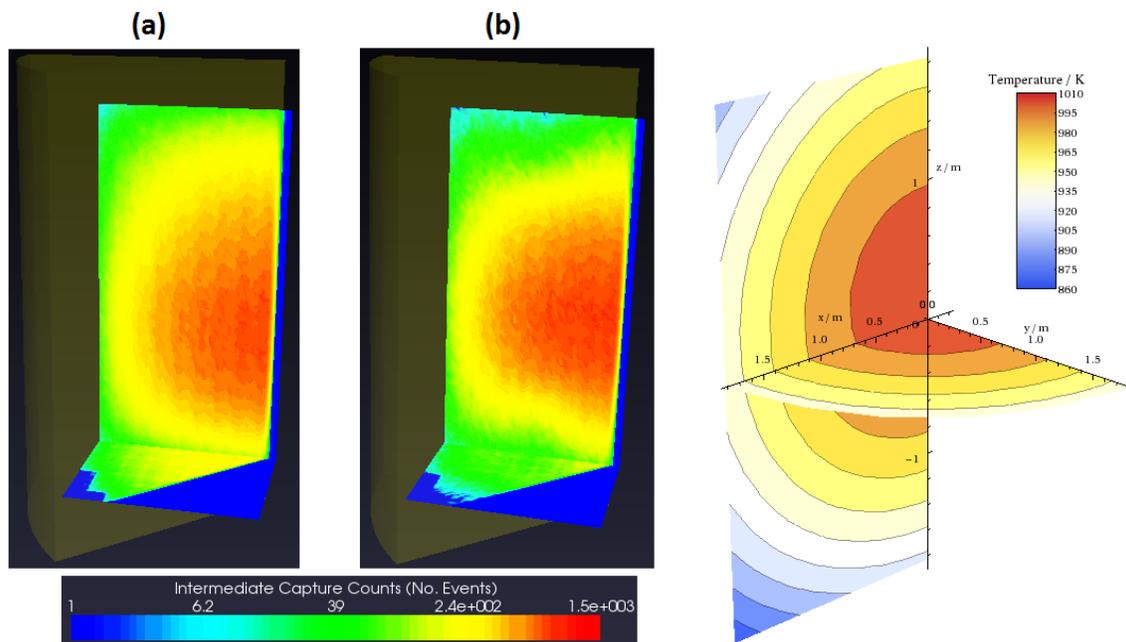
Figure 5: Axial and radial averages of intermediate capture events across the Hoogenboom and Martin benchmark 1/8th core model; (a) fixed temperatures and (b) estimated temperature profile. Estimated temperature profile across the core in the axial and radial directions is shown far right.

The calculations were performed with 100 settling stages and 200 scoring stages, using 50,000 samples per stage. The calculated k-effective values for the average fixed temperature and varying temperature profile cases were 1.0134 and 1.0350 respectively, a significant difference of the order 2000 pcm.

Differences in reactivity due to on-the-fly Doppler broadening can also be demonstrated using the new AT-in-UT module. Here the number of capture events in the intermediate energy range (from 0.4 eV to

0.1 MeV) for both the fixed and varying temperature profile cases were scored. Scored tallied results, averaged in the axial and radial directions, superimposed onto the VisualWorkshop wireframe view can be seen in Fig. 5. The impact of on-the-fly Doppler broadening on the reactivity in the intermediate energy range is seen by the differences between the number of capture events for the two temperature cases, where the varying profile case has increased counts in the central region of the core where temperatures are higher than the average fixed values. This is expected as the degree of Doppler broadening will increase with temperature and lead to increased intermediate energy capture (through flattening of resonant energy peaks in this range). Conversely, the varying temperature profile case has reduced capture events in the outer regions of the core where temperatures are lower than the average fixed values.

8. Conclusions

MONK10A is a major new release of the UK nuclear industry standard Monte Carlo code for nuclear criticality analysis. It features an extensive list of new and improved capabilities to assist the criticality analyst and improve the physical predictions of criticality calculations, some of which have been described in this paper. The runtime performance of MONK10A has been improved compared to MONK9A, with MONK10A on average being 2.4 times faster. Further increases in the performance of MONK10A can also be achieved using the new parallel capability.

Amongst the enhancements to geometry package is the capability to import CAD models in a variety of different ways including: IGES files as generated by CAD packages such as Solidworks or Autodesk Inventor; triangular polygon surfaces in STL and OBJ file formats; and tetrahedral meshes. To demonstrate these capabilities a fuel transport flask has been modeled in the native MONK Fractal Geometry package, as well as by importing IGES, polygon surface and tetrahedral mesh representations. These cases demonstrate good agreement, provided sufficient resolution is used in the POLY and TETMESH cases to adequately represent the curved surfaces.

The new Unified Tally module provides the capability to define any number of tally bodies, each with their own energy group scheme for scoring neutron scalar flux. The tally bodies may also be used for scoring action tallies of various reactions using AT-in-UT, allowing the user to analyze and interpret the underlying reactor physics of a calculation for specific regions within a model or by individual material compositions or nuclides. Tally bodies also permit the calculation of Shannon entropy for the scalar neutron flux to establish source convergence, as demonstrated by the fuel transport flask example, giving the user increased confidence that enough settling stages of a calculation have been performed to remove biases from an insufficiently converged source.

Comparisons of the new BINGO data libraries available in MONK10A show good agreement across a range of typical fissile and moderator materials, with largest differences found when using [241]Pu. The ability to adjust individual cross-sections of a BINGO library and calculate the sensitivity of k-effective to $\bar{v}$ for specific fissile materials has also been demonstrated. Finally, the impact of on-the-fly Doppler broadening within BINGO data libraries (performed at up to temperatures of 80,000 K) on both k-effective and reactions rates has been demonstrated using a PWR core model.

REFERENCES

1. S. D. Richards et al., "MONK and MCBEND: Current status and recent developments," *Annals of Nuclear Energy*, (2014).
2. F. B. Brown, "A review of Monte Carlo criticality calculations - convergence, bias, statistics", *International Conference on Mathematics, Computational Methods & Reactor*

Physics (M&C 2009), Saratoga Springs, New York, May 3-7, 2009, on CD-ROM, American Nuclear Society, LaGrange Park, IL (2009).

3. F. B. Brown, "A Review of Best Practices for Monte Carlo Criticality Calculations", *ANS Nuclear Criticality Safety Topical Meeting*, Richland, WA, 13-17 September 2009, LA-UR-09-03136, (2009).

4. C. E. Shannon, "A mathematical theory of communication", *The Bell System Technical Journal*, **27**, pp.623-656, (1948).

5. F. B. Brown, "Convergence testing and acceleration in MCNP5 criticality calculations," *Proc. 8th International Conference on Nuclear Criticality Safety*, p.356–359, St. Petersburg, Russia (2007).

6. A. Bird and A. Kyrieleis, "Experience Using Models Imported From CAD Software for Shielding Calculations In MCBEND," *Proc. 12th International Conference on Radiation Shielding (ICRS-12) and 17th Topical Meeting on Radiation Protection and Shielding (RPSD-2012)*, Nara, Japan, 2012.

7. K. Searson, F. Fleurot, A. Cooper and P. Cowen, "Importing CAD Models into MONK and MCBEND," *Computational Methods & Reactor Physics (M&C 2009)*. Saratoga Springs, New York (2009).

8. T. Barker, A. Bird, R. Thetford and A.J. Cooper, "Use of tetrahedral mesh geometry to import a converted CAD file for shielding and criticality calculations with MONK and MCBEND," *Proc. 11th International Conference on Radiation Shielding (ICRS-11) and 14th Topical Meeting on Radiation Protection and Shielding (RPS 2008)*,Georgia, USA (April 2008).

9. Dyrda, J., "Development of benchmarks for historical UK IEU criticality experiments and analysis using a Kalman filter data assimilation technique," *Diss. Imperial College London*, (2013).

10. Dean, C., et al., "Validation of Run-time Doppler Broadening in MONK with JEFF3. 1," *Journal of the Korean Physical Society*, **59.2**, pp.1162-1165, (2011).

11. J. E. Hoogenboom, W. R. Martin and B. Petrovic, "Monte Carlo performance benchmark for detailed power density calculation in a full size reactor core benchmark specifications," *Ann Arbor,* **1001**, (2010).